The Astrophysical Journal, 701:1415–1425, 2009 August 20 doi:10.1088/0004-637X/701/2/1415

Ne ISOTOPES IN INDIVIDUAL PRESOLAR GRAPHITE GRAINS FROM THE MURCHISON METEORITE TOGETHER WITH He, C, O, Mg-Al ISOTOPIC ANALYSES AS TRACERS OF THEIR ORIGINS

Philipp R. Heck[1,5], Sachiko Amari[2], Peter Hoppe[1], Heinrich Baur[3], Roy S. Lewis[4], and Rainer Wieler[3]
[1] Max-Planck-Institute for Chemistry, Particle Chemistry Department, J.-J.-Becherweg 27, D-55128, Mainz, Germany; prheck@gmail.com, prheck@uchicago.edu
[2] Laboratory for Space Sciences and the Physics Department, Washington University, Campus Box 1105, One Brookings Drive, St. Louis, MO 63130, USA
[3] ETH Zurich, Isotope Geology and Mineral Resources, Clausiusstr. 25, NW C84, CH-8092 Zurich, Switzerland
[4] Enrico Fermi Institute and Chicago Center for Cosmochemistry, The University of Chicago, Chicago, IL 60637, USA
Received 2008 October 20; accepted 2009 June 23; published 2009 July 31

ABSTRACT

Ne isotopes measured in individual presolar graphite grains, solid samples of extinct stars preserved in primitive meteorites, provide information on the type of stellar sources of the grains and on nucleosynthetic mixing and ion-trapping processes which were operating. We present Ne and He isotope analyses of single presolar graphite grains from the KFB1 density fraction extracted from the carbonaceous chondrite Murchison. In addition, we measured isotopes of C, O, and Mg-Al with the NanoSIMS ion microprobe to better constrain the origin of the grains. Eleven out of 51 presolar graphite grains contain nucleosynthetic ^{22}Ne above our detection limit. This fraction of ^{22}Ne-rich grains is similar to the one reported by Nichols et al. although we have a lower ^{22}Ne detection limit. We detected rare He-shell ^{20}Ne in one ^{22}Ne-rich grain and obtained the ^{20}Ne/^{22}Ne ratio (0.03 ± 0.02) of the He-shell of an Asymptotic Giant Branch (AGB) star with 1.5–2 $M_{\odot}$ and subsolar metallicity. We also detected ^{4}He in this grain, while in the other grains, which originally acquired He, He-loss seems to be significant. We found unequivocal evidence for radiogenic ^{22}Ne (Ne-R) in another graphite grain, which likely condensed in a core-collapse supernova and which incorporated live radioactive ^{22}Na ($t_{1/2} = 2.6$ yr). For the other grains, a clear assignment to a stellar source is more difficult to make. Putative stellar sources are supernovae, AGB stars, born-again AGB stars, J-type carbon stars, and CO novae.

Key words: circumstellar matter – dust, extinction – methods: analytical – methods: laboratory – nuclear reactions, nucleosynthesis, abundances

1. INTRODUCTION

Isotopically highly anomalous neon was discovered by Black & Pepin (1969) in carbonaceous chondrites. This neon, highly enriched in its heaviest isotope ^{22}Ne and named Ne-E, was assigned to a circumstellar source. This anomalous Ne component later led to the discovery and isolation of its carrier phase presolar graphite, primarily round grains >1 μm in diameter (Amari et al. 1990). The primary motivations for laboratory investigations of presolar graphite are to elucidate their stellar sources, to investigate nucleosynthetic processes, and to study dust condensation around stars.

Noble gas studies of different density fractions of bulk samples of millions of presolar graphite grains isolated from the carbonaceous chondrite Murchison (Amari et al. 1995) revealed that the samples actually contained two different ^{22}Ne-rich components. One component, released from the bulk samples during analysis at low temperature heating steps, was named Ne-E(L). The second one, released at high-temperature steps, was named Ne-E(H) (Eberhardt et al. 1981) and is slightly less ^{22}Ne-rich than the former. Subsequent work (Amari et al. 1995) found that Ne-E(L) released from the millions of grains actually consists itself of two distinct components: mainly radiogenic Ne-R (^{22}Ne from the decay of radioactive ^{22}Na, $t_{1/2} = 2.6$ yr; Clayton 1975) as well as a minor contribution of nucleosynthetic Ne-G, produced in the He-shell in Asymptotic Giant Branch (AGB) stars (Gallino et al. 1990, [^{20}Ne/^{22}Ne]-G $\approx 3 \times 10^{-2}$ to 1×10^{-1}, Heck et al. 2007) carried by a different population of grains. In contrast, the component Ne-E(H) exclusively consists of Ne-G. In this study, we only use the pure endmember components Ne-G and Ne-R. Na-22 is produced in supernovae and novae (Clayton 1975; Clayton & Hoyle 1974). Graphite grains from density fractions where Ne-R has been detected have ^{18}O excesses and Si isotopic anomalies (mainly in the form of ^{28}Si excesses). This leads to the assumption that many of the graphite grains originated in supernova explosions. Subsequent studies pointed out that novae only play a minor role as sources for graphite (e.g., Amari 2006). Gehrz et al. (1998) estimated that novae contribute only 3‰ to the interstellar dust inventory. The work on bulk samples showed that the original Ne isotopic composition acquired in a presolar, stellar environment has been largely preserved in presolar graphite.

To constrain the graphite's origin further, it is important to know the isotopic composition of noble gases as well as other diagnostic nuclides from individual grains. Helium and Ne analyses of single presolar graphite grains from Murchison were pioneered by Nichols et al. (1992). They discovered that in the density fraction KFB1 from Murchison (2.10–2.15 g cm^{-3}), ~29% of the presolar graphites (14 out of 49 grains) contained measurable amounts of ^{22}Ne. This is the same density fraction studied again in this work. In the low-density fraction KE3 (1.65–1.72 g cm^{-3}), Nichols et al. (1994) found a similar proportion (33%; 7 out of 21 grains) of ^{22}Ne-rich grains, while in the higher density fraction KFC1 (2.15–2.20 g cm^{-3}), only ~7% of the grains (3 out of 46 grains) are ^{22}Ne-rich (Kehm et al. 1996). None of the grains studied by these authors revealed the presence of any ^{20}Ne, ^{21}Ne, or ^{4}He above their detection limits. The most gas-rich grains account for most of the total gas amount. It remains an open question whether the Ne-R

[5] Present address: Chicago Center for Cosmochemistry and Department of the Geophysical Sciences, The University of Chicago, Chicago, IL 60637, USA.

was implanted into the grains after they formed or whether the Ne-R precursor nuclide ^{22}Na was incorporated into the grains during their condensation (e.g., Amari 2006; Amari 2009). It also remains elusive whether the grains with no noble gases detected never acquired any gas or the gas amounts are simply below detection limits.

A large database of C, N, O, Mg-Al, Si, and Ca-Ti isotopes of single presolar graphite grains was obtained by Hoppe et al. (1995) and Travaglio et al. (1999). It has been observed that each graphite density fraction has its own isotopic and trace element characteristics and hence represents a distinct mixture of products from different stellar sources. For example, in low-density graphite grains, nucleosynthetic signatures are preserved in the isotopes of C, O, Si, and N, while in high-density graphite grains, O and N show normal composition which is most likely due to equilibrium exchange with solar/terrestrial O and N. Radiogenic ^{26}Mg, ^{41}K, and ^{44}Ca (from the short-lived radionuclides ^{26}Al, ^{41}Ca, and ^{44}Ti, respectively) were detected in several graphite grains (Hoppe et al. 1995; Nittler et al. 1996; Amari et al. 1996; Travaglio et al. 1999). These analyses suggest that core-collapse supernovae (Type II) play an important role as sources particularly of low-density presolar graphite. In contrast, more high-density grains (KFC1 density fraction) bear signatures, e.g., the chemical composition of internal refractory carbides and the isotopic compositions of heavy elements, from AGB stars (e.g., Croat et al. 2005; 2008). The isotopic compositions of a few grains are qualitatively consistent with a nova origin (Amari et al. 2001a; José & Hernanz 2007).

Presolar ^{22}Ne without any detectable amounts of ^{20}Ne has also been observed in single presolar SiC grains from the carbonaceous chondrites Murchison (Nichols et al. 1992; Heck et al. 2007) and Murray (Heck et al. 2007), where it was mostly accompanied by ^{4}He. This information, together with C, N, and Si isotopic data of these grains, indicated that in contrast to presolar graphite, most of the SiC grains condensed in the outflows of low-mass AGB stars and the noble gases were implanted later by a fast stellar wind in the post-AGB phase (Heck et al. 2007). Only 1% of presolar SiC formed in supernovae (e.g., Amari et al. 1992; Hoppe et al. 2000). It is still an open question why the fraction of presolar graphite grains with a likely supernova origin is distinctly higher than that of presolar SiC grains (Zinner 2004).

In this study, we aim to determine the fraction of ^{22}Ne-rich graphite grains with the advantage of a higher Ne-sensitivity compared with the first study of noble gases in single graphite grains (Nichols et al. 1992). Rare gas analyses of single micron-sized presolar gains are very challenging due to the extremely small gas amounts. Furthermore, we investigate the grain-size dependency of the Ne concentration to shed light on the trapping mechanism of Ne into presolar graphite. One of our main goals is also to search for the rare, previously not detected ^{20}Ne and ^{4}He in individual presolar graphite grains. The Ne isotopic composition (i.e., the ^{20}Ne/^{22}Ne ratio), in conjunction with other isotope systems, is useful to to discern between supernova, nova, and AGB star origins, and in particular to distinguish between different nova types. We compare the light noble gas composition, together with isotopic data of C, O, and Mg-Al, with stellar nucleosynthetic model predictions to better constrain the stellar sources of gas-rich presolar graphite grains. Such an approach is only possible with single grain analyses.

Table 1
He and Ne detection limits (10^{-15} cm^3 STP) of the three noble gas analysis sessions. Data from session 1 have been rejected due to the high ^{4}He, ^{20}Ne, and ^{22}Ne detection limits

	^{4}He	^{20}Ne	^{21}Ne	^{22}Ne
Session 1	1300	60	0.51	6.2
Session 2	230	31	0.27	3.6
Session 3	230	0.33	37	1.7

2. SAMPLES AND EXPERIMENTS

Presolar graphite was extracted from Murchison at the University of Chicago using an acid dissolution and density separation technique described by Amari et al. (1994). Graphite grains from the acid residue of the KFB1 density fraction (2.10–2.15 g cm^{-3}) were mounted on ultraclean Au-foil and imaged in the secondary electron microscope (SEM). Thereafter, secondary ions ^{12}C$^-$, ^{13}C$^-$, ^{16}O$^-$, ^{18}O$^-$, and ^{28}Si$^-$ from 134 selected grains were analyzed in multicollection mode using a Cs$^+$ primary ion beam with the NanoSIMS ion-microprobe at Washington University in St. Louis. Special care was taken to consume only small sample amounts in order to provide enough material for subsequent rare gas analyses. The primary beam was rastered over the exposed grain surface (2×2 μm^2 and 3×3 μm^2 raster fields). The measurement was stopped when uncertainties of C isotope ratios based on counting statistics were better than 1%. A previous study suggests that short NanoSIMS analyses of major element isotopes do not have a detectable effect on the noble gas concentrations (Heck et al. 2007). Sixty presolar graphite grains (ø 1.7–6.2 μm), with a spatial separation to their neighbors considerably larger than the laser beam spot diameter ($\sim$50 μm), were analyzed for He and Ne isotopic composition at ETH Zurich. Gases were extracted by melting single grains with an Nd-YAG IR laser. The glowing of the grains was monitored with a video camera and reached its maximum intensity usually in less than one minute of continuous energy increase. After gas cleaning with getters and cold traps the sample gas was pumped almost quantitatively into the ion-source by a special-purpose molecular drag pump to achieve high sensitivity (Baur 1999). The He-4$^+$, ^{20}Ne$^+$, ^{21}Ne$^+$, and ^{22}Ne$^+$ as well as interfering ions were detected with an electron multiplier in ion-counting mode using peak jumping. For each measurement the instrument's memory and background signals were recorded and subtracted from the sample data. Our detection limits—defined by the 2σ scatter of blank measurements—for the three analyses sessions are given in Table 1. This procedure has been developed for the analyses of individual presolar SiC grains. A more detailed description is given by Heck et al. (2007). Data from the first analysis session were discarded due to the high scatter of the blank data. We subsequently focus on the data of 51 grains from sessions 2 and 3 (Figure 1, Tables 2 and 3).

After noble gas analyses, the melt residues of the grains were imaged in the SEM at the MPI for Chemistry in Mainz to verify whether grains had been completely melted, and neighboring grains were checked whether they had remained unaffected by the laser beam.

Thirteen of 51 melt residues of graphite grains which completely melted but still contained large enough amounts of material for ion microprobe study (Figure 2) were selected for analysis of the diagnostic isotope system Mg-Al. The secondary ions ^{24}Mg$^+$, ^{25}Mg$^+$, ^{26}Mg$^+$, and ^{27}Al$^+$ were measured in

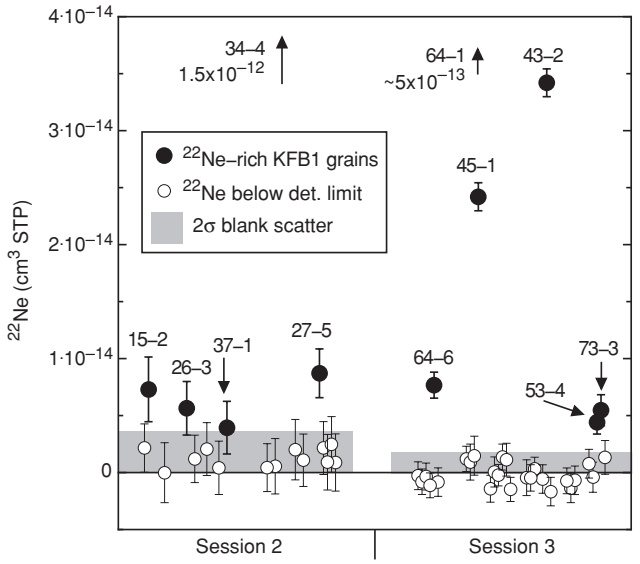

Figure 1. ^{22}Ne gas amounts of presolar graphite grains from the KFB1 density fraction from Murchison during two analysis sessions. The average blank value has been subtracted from the data. Detection limits are defined by the 2σ scatter of blank data of one session. Data from the first session have been rejected due to a high detection limit. Error bars on data points in all figures are 1σ and include analytical errors. 1 cm^3 STP = 2.6868×10^{19} atoms.

multicollection mode with the NanoSIMS in Mainz using a primary O^- beam. Due to the limited amount of material left in the melt residue, we have chosen to measure the Mg-Al isotopes instead of Ca-Ti isotopes since Al has a relatively high abundance in presolar graphite. Previous work has shown that presolar spinel grains have on average δ^{25}Mg ≈ 0‰ (Zinner et al. 2005). We have assumed an average δ^{25}Mg = 0‰ for the graphite grains here as well. The observed difference in the measured average ^{25}Mg/^{24}Mg ratios between our graphite grains and the Burma spinel standard of –34‰ to –37‰ amu^{-1} (depending on the measurement session) has been interpreted to be due to instrumental mass fractionation (matrix effects, sample topography, etc.) and Mg isotope ratios were corrected accordingly. Extinct ^{26}Al was inferred from excess ^{26}Mg, which is considered to be entirely radiogenic, using the following expression (Hoppe et al. 1995):

$$\left(\frac{^{26}\mathrm{Al}}{^{27}\mathrm{Al}}\right)_{\mathrm{inferred}} = \frac{\delta^{26}\mathrm{Mg}}{1000} \times \left(\frac{^{26}\mathrm{Mg}}{^{24}\mathrm{Mg}}\right)_{\mathrm{terrestrial}} \times \left(\frac{^{24}\mathrm{Mg}}{^{27}\mathrm{Al}}\right)_{\mathrm{measured}} \times \varepsilon, \quad (1)$$

where δ^{26}Mg is the sample's permill-deviation[6] from the terrestrial values $(^{26}\mathrm{Mg}/^{24}\mathrm{Mg})_{\mathrm{terrestrial}} = 1.3932 \times 10^{-1}$ and the sensitivity factor $\varepsilon = (\mathrm{Al}^+/\mathrm{Mg}^+)/(\mathrm{Al}/\mathrm{Mg}) = 1.17$ was derived by comparing the measured ratio of the standard with its true ratio.

3. RESULTS

3.1. C and O Isotopes

The ^{12}C/^{13}C ratios range from 4 to 1300 (^{12}C/^{13}C$_\odot$ = 89). Except for two grains, which differ from solar composition by slightly more than 2σ, the ratios of all other grains are distinct from solar by $>4\sigma$. From the carbon isotopic compositions alone we can conclude that the grains are of extrasolar origin. Ten graphite grains for which noble gases were measured have relatively low ^{12}C/^{13}C ratios (<16). One of these grains is KFB1g 45-1 with both ^{22}Ne and ^{20}Ne above detection limit (see below). Six of the other grains have ratios ^{12}C/^{13}C < 10, with three of them containing ^{22}Ne above detection limit. The ^{16}O/^{18}O ratios range from 300 to 550 (^{16}O/^{18}O$_\odot$ = 499), but are normal within error for most of the samples. Hoppe et al. (1995) and Croat et al. (2008) concluded that the O-isotopic composition reflects dilution with normal O at some time after grain formation. The dilution process probably occurred in the solar nebula, in the parent asteroid, and in the laboratory. The ^{12}C/^{13}C and ^{16}O/^{18}O ratios for grains where noble gases were measured are given in Table 3.

3.2. Ne Isotopes

Eleven graphite grains out of the 51 grains analyzed in two sessions contain ^{22}Ne above our detection limits (see Figure 1; Table 3). This fraction (22%), while smaller, is statistically indistinguishable from Nichols et al.'s (1992) fraction of ^{22}Ne-rich grains (30%; 14 out of 49 grains) for the same density fraction. We detected for the first time ^{20}Ne in an individual graphite grain and could determine the ^{20}Ne/^{22}Ne ratio (KFB1g 34-4: ^{20}Ne/^{22}Ne = [3.2 ± 1.8] × 10^{-2}). If not mentioned otherwise, all errors are given as 1σ and include analytical uncertainties based on counting statistics. For grains containing only ^{22}Ne above detection limit, upper limits of the ^{20}Ne/^{22}Ne

[6] $\delta^A\mathrm{Mg} = \left(\frac{(^A\mathrm{Mg}/^{24}\mathrm{Mg})_{\mathrm{sample}}}{(^A\mathrm{Mg}/^{24}\mathrm{Mg})_{\mathrm{standard}}} - 1\right) \times 10^3$.

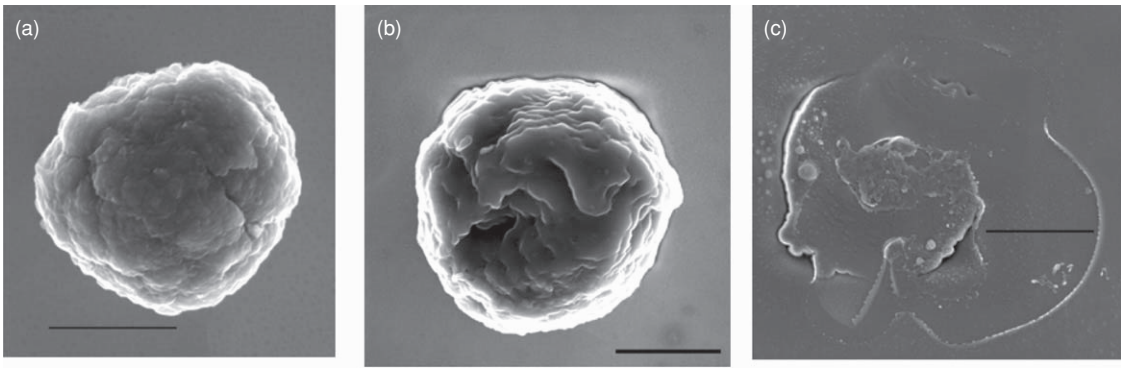

Figure 2. SEM images of three different KFB1 graphite grains showing their typical appearance (a) after physiochemical separation from the meteorite matrix, (b) after surface sputtering due to NanoSIMS analyses, and (c) after IR laser melting for extraction of noble gases. The melt residue has about the same size as the unmelted grain and still allowed detection of significant amounts of Mg-Al isotopes using the NanoSIMS. The black scale bar is 1 μm in length.

Table 2
Isotope Ratios of KFB1g Graphite Grains

Grain KFB1g-	Gas-rich?	ø[μm]	$^{12}C/^{13}C$	$^{20}Ne/^{22}Ne$	$\delta^{25}Mg$(‰)	$(^{26}Al/^{27}Al)_{inferred}(10^{-3})$	$^{16}O/^{18}O$	Putative stellar source
64-1[b]	^{22}Ne	5.18	485.7 ± 4.4	⩽0.0007			503.2 ± 21.2	Supernova
34-4[a]	$^{20,22}Ne$, ^{4}He	2.17	98.2 ± 0.8	0.032 ± 0.018	30 ± 22	6.34 ± 0.89	488.8 ± 20.8	AGB star or less likely supernova
45-1[b]	$^{20,22}Ne$	3.73	15.9 ± 0.1	1.7 ± 1.0	−75 ± 33	⩽0.56	495.2 ± 18.8	Supernova?
26-2[a]		3.65	28.6 ± 0.2		24 ± 29	2.64 ± 1.25	301.8 ± 9.3	Supernova?
15-2[a]	^{22}Ne	6.18	10.4 ± 0.1	⩽8.6	−15 ± 22	8.17 ± 0.86	512.6 ± 18.6	Born-again AGB star? Supernova?
10-1[a]		1.94	13.7 ± 0.1		−98 ± 29	⩽0.076	508.4 ± 20.5	J-type C-star?
43-2[b]	^{22}Ne	2.36	9.0 ± 0.1	⩽0.01	35 ± 123	⩽2.0	529.4 ± 25.3	Born-again AGB star or supernova?
73-3[b]	^{22}Ne	1.88	8.6 ± 0.1	⩽0.1	39 ± 125	⩽3.7	540.7 ± 33.8	Born-again AGB star, CO nova, or Supernova?
53-2[b]		3.31	4.7 ± 0.0		101 ± 107	⩽0.98	510.5 ± 26.5	J-type C-star or CO nova?
56-1[b]		3.62	4.0 ± 0.0				491.0 ± 17.6	J-type C-star or CO nova?
57-3[b]		2.21	5.0 ± 0.0				527.7 ± 17.9	J-type C-star or CO nova?
26-3[a]	^{22}Ne	2.21	1305.1 ± 14.7	⩽8.6	16 ± 27	3.22 ± 0.89	512.4 ± 21.0	AGB star or supernova?
53-4[b]	^{22}Ne	2.24	246.1 ± 2.3	⩽0.1	−9 ± 23	1.38 ± 0.53	510.8 ± 33.8	
64-6[b]	^{22}Ne	3.18	623.3 ± 5.8	⩽0.06			526.8 ± 21.2	
27-5[a]	^{22}Ne	1.78	693.4 ± 8.0	⩽7.0	−104 ± 27		542.5 ± 33.6	
37-1[a]	^{22}Ne	3.82	857.1 ± 8.6	⩽8.6	6 ± 47	⩽2.8	510.3 ± 27.9	
07-1[a]		4.37	341.9 ± 3.0				529.1 ± 21.2	
12/22-1/1[a]		1.75	201.3 ± 1.7		−26 ± 22	⩽0.23	525.2 ± 19.6	
24-2[a]		1.97	512.3 ± 4.9		84 ± 53	3.92 ± 1.49	531.9 ± 25.3	
25-3[a]		2.58	965.3 ± 9.7		33 ± 22	0.16 ± 0.02	499.2 ± 24.4	
27-1[a]		2.75	87.0 ± 0.7				486.2 ± 18.3	
30-1[a]		2.58	842.6 ± 8.7		−16 ± 24	5.55 ± 1.48	553.7 ± 35.2	
30-2[a]		1.96	502.0 ± 4.7				479.3 ± 20.9	
31-1[a]		3.16	118.7 ± 1.0				513.7 ± 21.0	
31-2[a]		2.24	1064.1 ± 11.0				527.1 ± 33.4	
32-1[a]		3.05	212.1 ± 1.8				506.1 ± 19.2	
32-2/3[a]		1.89	98.3 ± 0.8		46 ± 25	1.27 ± 0.34	478.4 ± 26.2	
40-1[b]		2.65	1028.8 ± 10.4				525.2 ± 29.3	
41-1[b]		2.30	560.1 ± 5.1				514.8 ± 29.3	
42-1[b]		2.03	642.9 ± 6.2				500.2 ± 19.2	
43-1[b]		2.41	374.9 ± 3.5				516.1 ± 24.4	
43-3[b]		2.00						
45-2[b]		2.99	1159.6 ± 11.7				530.5 ± 24.9	
46-1[b]		3.77	13.0 ± 0.1				481.4 ± 17.1	
51-1[b]		2.53	147.3 ± 1.2		−7 ± 58	⩽0.43	504.8 ± 19.9	
51-2[b]		2.20	86.3 ± 0.7		43 ± 27	⩽0.15	522.4 ± 21.4	
53-1[b]		2.28	396.5 ± 3.6				515.8 ± 20.9	
57-1[b]		2.74	45.3 ± 0.4				505.0 ± 16.2	
58-1[b]		4.65	16.2 ± 0.1				447.8 ± 16.4	
61-1[b]		3.90	217.5 ± 1.9				526.3 ± 22.3	
62-1[b]		4.17						
63-1[b]		3.09	87.3 ± 0.7		57 ± 25	0.62 ± 0.17	503.0 ± 18.0	
63-4[b]		2.70						
64-4[b]		1.68	453.1 ± 4.5				486.9 ± 17.3	
65-1[b]		1.84	60.8 ± 0.5				496.4 ± 24.0	
71-1[b]		4.08	592.0 ± 6.1				529.9 ± 31.0	
71-2[b]		1.87	552.5 ± 5.4				507.4 ± 22.3	
73-1[b]		3.29	1074.7 ± 12.0				524.0 ± 31.5	
73-2[b]		2.69	761.1 ± 7.9				535.7 ± 26.5	

Notes. Isotope ratios of KFB1g graphite grains for which noble gases have been measured and their most likely stellar sources. We first list grains where one likely parent star type has been assigned, followed by grains where different types of stellar sources are possible. Uncertainties are 1σ analytical errors.
[a] Noble gas analysis session 2. [b] Noble gas analysis session 3.

Table 3
Gas Amount and Concentrations of ^{22}Ne-rich KFB1g Graphite Grains and Upper Limits of ^{20}Ne/^{22}Ne Ratios of the Other Grains

Grain KFB1g-	Diameter (μm)	^{22}Ne (10^{-14} cm^3 STP)	[^{22}Ne] (10^{-3} cm^3 STP g^{-1})	^{20}Ne/^{22}Ne
07-1[a]	4.37			
10-1[a]	1.94			
12/22-1/1[a]	1.75			
15-2[a]	6.17	0.73 ± 0.28	0.028 ± 0.011	⩽8.6
24-2[a]	1.97			
25-3[a]	2.58			
26-2[a]	3.65			
26-3[a]	2.21	0.56 ± 0.23	0.47 ± 0.20	⩽8.6
27-1[a]	2.75			
27-5[a]	1.78	0.87 ± 0.21	1.39 ± 0.34	⩽7.0
30-1[a]	2.58			
30-2[a]	1.96			
31-1[a]	3.16			
31-2[a]	2.24			
32-1[a]	3.05			
32-2/3[a]	1.89			
34-4[a]	2.17	145.00 ± 0.71	128.0 ± 1.6	0.032 ± 0.018
37-1[a]	3.82	0.39 ± 0.23	0.064 ± 0.037	⩽8.6
40-1[b]	2.65			
41-1[b]	2.30			
42-1[b]	2.03			
43-1[b]	2.41			
43-2[b]	2.36	3.42 ± 0.12	2.340 ± 0.088	⩽0.01
43-3[b]	2.00			
45-1[b]	3.73	2.42 ± 0.12	0.419 ± 0.022	1.7 ± 1.0
45-2[b]	2.99			
46-1[b]	3.76			
51-1[b]	2.53			
51-2[b]	2.20			
53–1[b]	2.28			
53-2[b]	3.31			
53-4[b]	2.24	0.44 ± 0.10	0.354 ± 0.084	⩽0.1
56-1[b]	3.62			
57-1[b]	2.74			
57-3[b]	2.21			
58-1[b]	4.65			
61-1[b]	3.90			
62-1[b]	4.17			
63-1[b]	3.09			
63-4[b]	2.70			
64-1[b]	5.18	48.40 ± 0.25	3.140 ± 0.040	⩽0.0007
64-4[b]	1.68			
64-6[b]	3.18	0.77 ± 0.11	0.215 ± 0.032	⩽0.06
65-1[b]	1.84			
71-1[b]	4.08			
71-2[b]	1.87			
73-1[b]	3.29			
73-2[b]	2.69			
73-3[b]	1.88	0.55 ± 0.14	0.74 ± 0.18	⩽0.1

Notes. Uncertainties are 1σ analytical errors.
[a] Noble gas analysis session 2. [b] Noble gas analysis session 3.

ratio were determined (Table 3) as follows:

$$\left(\frac{^{20}\mathrm{Ne}}{^{22}\mathrm{Ne}}\right)_{\text{upper limit}} = \frac{^{20}\mathrm{Ne}_{\text{det.limit}}}{^{22}\mathrm{Ne}_{\text{measured}} - 2\sigma_{\text{error}}}. \quad (2)$$

This gives the highest possible ^{20}Ne/^{22}Ne ratio within 2σ uncertainty based on ion-counting statistics, a conservative estimate if only ^{22}Ne is known. We obtained a particularly low upper ^{20}Ne/^{22}Ne limit for grain 64-1 (^{20}Ne/^{22}Ne $\leqslant 7 \times 10^{-4}$) and low upper limits for grain 64-6 (^{20}Ne/^{22}Ne $\leqslant 6 \times 10^{-2}$) and for grains 43-2, 53-4, 73-3, and 53-4 (^{20}Ne/^{22}Ne $\leqslant 0.1$).

The ^{22}Ne amounts range from 3.9×10^{-15} to 1.5×10^{-12} cm^3 STP (standard temperature and pressure; 1 cm^3 STP = 2.6868×10^{19} atoms). Approximate ^{22}Ne concentrations range from 2.8×10^{-5} to 1.3×10^{-1} cm^3 STP g^{-1}. Concentrations were calculated by assuming spherical grains with a diameter being the average of the measured major and minor axes in SEM images of the grains. The concentration range partially overlaps

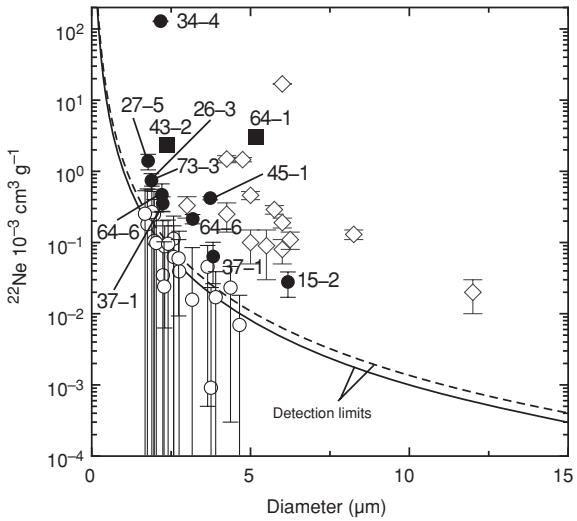

Figure 3. ^{22}Ne concentrations vs. grain size for single KFB1 graphite grains. Highest and lowest detection limits as a function of diameter are plotted as dashed and solid lines, respectively. Ne-22-rich grains are labeled solid circles. Open circles show data for samples with ^{22}Ne below our detection limit ("gas-poor"). For comparison, the KFB1 data obtained by Nichols et al. (1992) are plotted as open diamond symbols. The correlation with grain size observed for some grains in both data sets seems to imply a near-surface implantation of ^{22}Ne-G. Data points for Ne-R-containing grains 64-1 and 43-2 are shown as full squares.

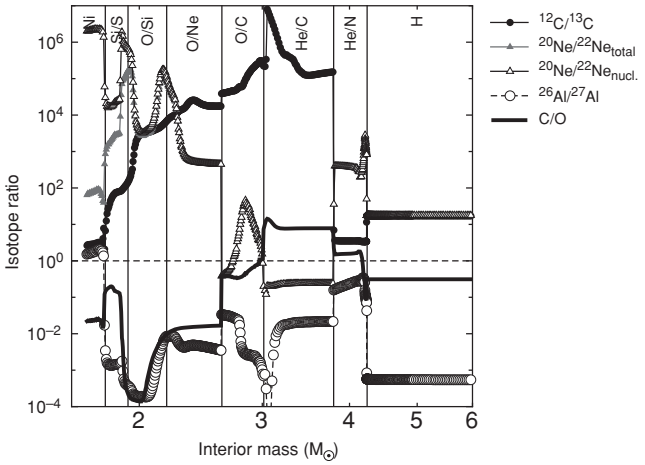

Figure 4. Profile of 15 $M_\odot$ supernova model (s15a28c) yields from Rauscher et al. (2002). All species indicated are expressed as ratios of nuclide number fractions and include decayed short-lived radioactive nuclides, e.g., yields for ^{22}Ne include decayed ^{22}Na and ^{26}Al yields include decayed ^{26}Si, ^{26,27}P, ^{26,27}S. The nucleosynthetic ^{20}Ne/^{22}Ne ratio is also shown without any contribution of radiogenic ^{22}Ne. Supernova zones, defined by the one or two most abundant elements, are separated by vertical lines. Source data are retrieved from nucleosynthesis.org.

the range found by Nichols et al. (1992) in grains from the same density fraction from Murchison (2.0×10^{-5} to 1.7×10^{-2} cm^3 STP g^{-1}). We find a rough correlation of decreasing ^{22}Ne-concentration with increasing grain size for some of the grains, based on the limited statistics (Figure 3; see Section 4.2 for discussion).

3.3. Helium-4

Helium-4 was detected for the first time in a single graphite grain (KFB1g 34-4). The ^{4}He concentration of this grain ([20.7 ± 12.7] × 10^{-3} cm^3 g^{-1}) is lower than the concentrations measured in most individual SiC grains (Nichols et al. 1992; Heck et al. 2007). The ^{4}He/^{22}Ne ratio of [8.4 ± 5.8] × 10^{-2} is several orders of magnitude lower than those determined in single SiC grains (Heck et al. 2007; see Section 4.1 for discussion) and also lower than ^{4}He/^{22}Ne of the terrestrial atmosphere (3.2×10^{-1}; Eberhardt et al. 1965; Mamyrin et al. 1970).

Note that He-4 was also detected during the analysis of grain 64-1. However, a large neighboring dust contamination glowed simultaneously during laser heating and possibly released terrestrial atmospheric ^{4}He. Although we observed a large amount of ^{22}Ne (~5×10^{-13} cm^3 STP) from this sample, we did not detect any ^{20}Ne. This excludes that terrestrial Ne has been released (^{20}Ne/^{22}Ne$_{air}$ = 9.8; Eberhardt et al. 1965) from the neighboring dust and implies that the ^{22}Ne measured in grain 64-1 is presolar.

3.4. Mg-Al Isotopes

The Mg-Al composition of 20 selected graphite grain melt residues was measured (Table 2). Values of δ^{25}Mg range from −104 ± 27 ‰ (grain 27-5) to 101 ± 107 ‰ (grain 53-2), with four grains having δ^{25}Mg ≠ 0 outside 2σ limits and values of δ^{26}Mg from −168 ± 27 ‰ (grain 27-5) to 213 ± 22 ‰ (grain 15-2). In 10 of 20 melt residues, we found ^{26}Mg excesses >2σ, which can be attributed to the decay of ^{26}Al. This allowed us to infer the original ^{26}Al/^{27}Al ratios, which range from (1.6 ± 0.2) × 10^{-4} (grain 25-3) to (8.2 ± 0.9) × 10^{-3} (grain 15-2). Upper limits on ^{26}Al/^{27}Al ratios could be calculated for nine other melt residues (⩽ 3.7×10^{-3}). The highest ratios found in this study are lower than the highest ones of ~1 × 10^{-1} found in KFB1 graphites by Hoppe et al. (1995). This might be partly due to the fact that we have measured melt residues instead of fresh grains. The inferred ^{26}Al/^{27}Al ratio could have been lowered by dilution with normal ^{27}Al, occurring as contamination in the sample mount.

Most grains (16 out of 20) have solar ^{25}Mg/^{24}Mg ratios within errors justifying the assumption of a solar initial ^{26}Mg/^{24}Mg ratio to calculate ^{26}Al/^{27}Al ratios. For grains 10-1, 27-5, and 45-1 with negative and nonzero δ^{25}Mg (with consideration of 2σ errors), inferred ^{26}Al/^{27}Al ratios may be very low because the initial ^{26}Mg/^{24}Mg ratio might have been subsolar as well. For these three grains we will discuss possible reasons for their low ^{25}Mg/^{24}Mg ratios.

4. DISCUSSION

Table 2 gives an overview of KFB1g graphite grains for which noble gas isotopes—if any—have been detected, in particular grains in this work. In the following, we will discuss what we learn from noble gases about the trapping mechanisms and possible stellar sources of presolar Ne and, in combination with isotope data of other elements, about the origins of presolar grains. The result of this discussion is summarized in the last column of Table 2. In a rather qualitative approach we compare the Ne data and isotopic compositions of the other elements measured with nucleosynthetic model predictions for supernovae, AGB stars, and novae, the most likely stellar sources of presolar graphite grains. Throughout the discussion, we refer to an onion shell supernova model from Rauscher et al. (2002), where we label different zones according to their most abundant elements, as first proposed by Meyer et al. (1995; see Figure 4).

Although we have detected He in one graphite grain, He has presumably been lost from most of the grains and has therefore limited diagnostic ability for most presolar graphite grains. This

stands in contrast to a higher fraction of He-rich presolar SiC grains (Heck et al. 2007). Nevertheless, the rarity of He in graphites deserves attention by itself.

4.1. Helium Implantation and Loss

Grain 34-4 is the first individual presolar graphite grain where He has been detected. The concomitant occurrence of ^{4}He, ^{22}Ne, and ^{20}Ne in this grain supports the idea of trapping through ion implantation. However, the low ^{4}He concentration and the very low ^{4}He/^{22}Ne ratio [8.4 ± 5.8] × 10^{-2} are unexpected from theoretical considerations. The ^{12}C/^{13}C ratio of 98 in grain 34-4 suggests an origin in an AGB star or a supernova explosion. If ion implantation occurred in a post-AGB star environment (^{4}He/^{22}Ne in mainstream SiC = 25–300, ^{4}He/^{22}Ne in AGB star models = 108–591; Heck et al. 2007), or in a supernova explosion (average ^{4}He/^{22}Ne in the He/C zone of 15 $M_\odot$ model is 691, in the He/N zone ^{4}He/^{22}Ne = 8.8×10^5, and in the H zone 19000; Rauscher et al. 2002; graphite is expected to condense mostly from matter from the He/C and He/N zones at equilibrium conditions; see Section 4.2.1), we would expect ^{4}He/^{22}Ne ratios at least to be 2–3 orders of magnitude higher than the observed values. Such low ^{4}He/^{22}Ne ratios can only be produced in the O/Ne zone of a supernova (15 $M_\odot$ model of Rauscher et al. 2002); however, the average ^{20}Ne/^{22}Ne ratio of this zone is 334 in the same model, clearly at odds with our grain data (^{20}Ne/^{22}Ne = ∼3 × 10^{-2}). We rule out that the low ratios were produced by fractionation during ion implantation: The stopping depths in graphite of He and Ne ions with the assumed post-AGB stellar wind energies ($E_{\mathrm{He-4}}$ = 200 ± 120 keV, $E_{\mathrm{Ne-22}}$ = 700 ± 350 keV) are smaller than the size of our samples (see Section 4.2). Ions with similar energies and also much faster ones could be produced in supernovae. According to SRIM simulations (Stopping and Range of Ions in Matter; Ver.2003.26; Ziegler 2004), most of the very high-energy ions would traverse the grains and the small remainder in the grain (a few ‰) would even result in an increased ^{4}He/^{22}Ne ratio. As this is in contrast to our observations, this clearly indicates that He is much more easily lost from presolar graphite grains than from SiC grains. The weak retentivity of graphite grains for He could explain the absence of He in most of the samples and the low ^{4}He/^{22}Ne ratio measured in grain 34-4. The He/Ne ratios also imply that Ne is much better retained than He. This is also suggested by Ne concentrations and gas amounts comparable to the ones detected in presolar SiC (Heck et al. 2007).

4.2. Ne Sources and Trapping Mechanisms

4.2.1. Radiogenic Ne in Graphite Grains from Type II Supernovae

In presupernova stars only the He-rich zones (He/C and He/N) in the outermost part fulfill the condition C/O ∼ 1 or larger, required for the formation of graphite in equilibrium conditions if C and O are much more abundant than Si and Ti (Ebel & Grossman 2001). The highest absolute ^{22}Na abundances, however, are found in the intermediate zones (e.g., the O/Ne zone). Therefore, ^{22}Na-derived Ne-R might only be expected in graphite under equilibrium condensation if mixing of He-rich zones with intermediate zones occurred. Mixing scenarios were calculated and discussed by Travaglio et al. (1999), and more recently by Yoshida (2007). They explained many observed isotope ratios of presolar graphite grains successfully, but the mixing remained not without problems for some grains. Here, we qualitatively evaluate a supernova origin for presolar grains by comparing the grain data with predicted yields from a 15 $M_\odot$ supernova model (Figure 4) from Rauscher et al. (2002). This model uses an adaptive reaction network and gives yields for isotopes from H to Po for core-collapse Type II supernovae. None of our grains data matches the predictions from equilibrium condensation of a single supernova zone. Therefore, we compare our grain data with mixed ejecta: We calculate isotopic ratios obtained by a simple incremental ad hoc mixing of the different supernova zones (Travaglio et al. 1999; Hoppe et al. 2000) using yields from the 15 $M_\odot$ Rauscher et al. (2002) supernova model. Although the latter approach does not take into account the complex mixing processes occurring during the explosion, it could successfully explain the isotopic compositions of many presolar graphite and SiC grains thought to originate in supernovae (Travaglio et al. 1999; Hoppe et al. 2000; Besmehn & Hoppe 2003). However, we also note that there are calculations and observations that do not support a large degree of mixing in supernova ejecta: (1) Supernova models by Nozawa et al. (2003) produce oxide dust grains only, when mixing the ejecta. Their models yield carbonaceous dust, together with silicates and oxides, only in unmixed ejecta. (2) Recent infrared observations of dust and gas in the galactic core-collapse supernova remnant Cassiopeia A suggest that the ejecta are largely unmixed. The distribution of gas and dust in the remnant is rather consistent with unmixed supernova models and only requires a small degree of mixing (Rho et al. 2008).

Clayton et al. (1999) introduced a model for graphite formation dominated by kinetic chemistry where the condition C/O >1 is not necessary for graphite to condense, hence suggesting the possible production of Ne-R at the site of graphite condensation. This scenario has been further investigated by an improved model by Deneault et al. (2006). Condensation calculations by Ebel & Grossman (2001) show that if CO molecules are suppressed to form, graphite condenses if C/O > ∼0.48 and if all molecules are suppressed, graphite can even form if C/O ≪1. We note here that the first ionization potential of Ne is ∼4 × higher (∼22 eV) than that of Na (∼5 eV), allowing Na ions to dominate over Ne in a certain energy range, even while ^{22}Na/^{22}Ne < 1. However, it seems unlikely that such a particular energy range could have been maintained in all the different supernovae that produced presolar graphite grains. It is rather likely that both Na and Ne were ionized during the supernova explosion. Thus, both elements could have been implanted into the grains.

Various trapping mechanisms for ^{22}Ne in presolar graphite have been proposed. One of the earliest proposed scenarios involved the condensing graphite grain incorporating radioactive ^{22}Na from a supernova or a nova, which then decayed in situ to ^{22}Ne (Clayton 1975). Although Na is a volatile element, it can be incorporated into graphite as atomic layers intercalated between many layers of graphite (Asher & Wilson 1958). This would lead to ^{22}Ne (Ne-R) concentration in layers throughout the grain volume. In contrast, a decrease of ^{22}Ne concentration with increasing grain size as observed for some ^{22}Ne-rich grains (Figure 3) is characteristic of surface-implanted gas. However, in Figure 3 the data point of grain 64-1 falls to the right of the trend defined by other gas-rich grains and is therefore consistent with the above outlined ^{22}Na-trapping scenario. Grains containing Ne-R may also be expected to show lower ^{20}Ne/^{22}Ne ratios. The upper limit of the ^{20}Ne/^{22}Ne ratio of grain 64-1 (based on the detection limit of ^{20}Ne) of 7 × 10^{-4} is lower than the lowest nucleosynthetic ^{20}Ne/^{22}Ne ratios from supernovae (Rauscher et al. 2002; Limongi & Chieffi 2003; Chieffi & Limongi 2004; see also Figure 4), novae (José et al. 2004), and AGB stars

(Heck et al. 2007). We thus conclude that ^{22}Ne in grain 64-1 is predominantly radiogenic. This observation is consistent with the assumption that due to low gas–grain velocities in the supernova ejecta, Ne was only implanted into the grains' outermost ∼30 nm thin layer, which was later sputtered away by grain–gas interactions in the supernova reverse shocks (Amari 2009). At least three reverse shocks are important for grain formation and processing in a supernova. The first one forms when the expanding shock experiences deceleration when moving through the H-envelope. The second reverse shock forms when the expanding ejecta encounters the formerly ejected stellar wind, and the third one forms because of the encounter of the expansion with the interstellar medium (e.g., Deneault et al. 2003). Reverse shocks increase the relative velocities between dust grains and gas as a function of grain size (e.g., Nozawa et al. 2007). Nath et al. (2008) calculated a lower limit of 1%–20% in the mass of silicate and graphite dust to be sputtered away by the reverse shocks in a supernova. Nozawa et al. (2007) calculated that 1-μm-sized carbon dust grains will be eroded by 0.7% in size by kinetic sputtering occurring in the reverse shocks with relative gas/grain velocities of ∼500–1300 km s^{-1}. The stopping depth in graphite of previously implanted Ne ions is smaller than the grain size studied (see Section 4.2) if we assume relative velocities between dust and gas of <2000 km s^{-1}. Sputtering could then partially or completely remove the layer of implanted Ne from the grains. The presence of Ne-R in grain 64-1excludes an AGB star origin since AGB stars do not produce ^{22}Na. Novae not only synthesize abundant ^{22}Na but also efficiently produce ^{13}C at the expense of ^{12}C through proton capture. This leads to very low ^{12}C/^{13}C ratios (<3) in nova ejecta (José et al. 2004), clearly inconsistent with the ^{12}C/^{13}C ratio (∼500) of grain 64-1. We therefore conclude that grain KFB1g 64-1 was produced in a mixture of supernova ejecta (e.g., O/Ne:O/C:He/C:He/N zone mixture ratios 0.01:0.01:0.31:0.66).

Another grain that may contain Ne-R is sample 43-2. The upper limit of its ^{20}Ne/^{22}Ne ratio (1×10^{-2}) is lower than predictions for AGB star He-shell Ne (Heck et al. 2007) and for Ne in different supernova zones (Figure 4). An AGB star origin for this grain is therefore unlikely, both based on the presence of Ne-R and the low ^{12}C/^{13}C ratio of nine. Mixing matter from He/N and H zones in a 15 $M_{\odot}$ supernova (Figure 4; Rauscher et al. 2002) in a ratio 30:1 yields a ^{12}C/^{13}C ratio of 10, compatible with the grain data. However, in this mixing scenario, ^{26}Al/^{27}Al is 0.15, about an order of magnitude higher than the grain's inferred ^{26}Al/^{27}Al ratio ($\leqslant 2 \times 10^{-2}$). Only consideration of ∼90% contaminating Al could explain the grain's data. An origin from a 15 $M_{\odot}$ supernova seems thus unlikely. However, it is beyond the scope of this paper to explore a wider range of supernova masses and metallicities, and at present a supernova origin cannot be completely ruled out for grain 43-2. The same conclusions can be drawn from the isotope data of grain 73-3 (^{12}C/^{13}C = 8.6, ^{26}Al/^{27}Al$_{\rm inferred} \leqslant 3.7 \times 10^{-3}$, ^{20}Ne/^{22}Ne $\leqslant$ 0.1; Figure 4) and grain 15-2 (^{12}C/^{13} C = 10.4, ^{26}Al/^{27}Al = 8.3 $\times 10^{-3}$; ^{20}Ne/^{22}Ne $\leqslant$ 8.6). Because of their low ^{12}C/^{13}C ratios and putative Ne-R, we discuss a different origin for these grains (15-2, 43-2, 73-3) in Section 4.2.3.

Can the isotopic composition of gas-rich grain 34-4 be explained by a supernova origin? The isotopic composition of this grain is only partially compatible with predictions of equilibrium condensation in supernova ejecta. Mixing calculations for a 15 $M_{\odot}$ supernova (Rauscher et al. 2002) result in C/O = 0.5, ^{12}C/^{13}C = 98, O isotope ratios within 20% of solar, and ^{26}Al/^{27}Al = 0.0068 by mixing matter from the O/C, He/C, He/N, and H zones in a ratio 0.47:0.09:0.3:0.71. This is in good agreement with the grain's data. However, it is difficult to explain the ^{20}Ne/^{22}Ne ratio [3.2 ± 1.8] × 10^{-2} as a mixture of Ne-R with supernova Ne. Even when invoking the lowest predicted nucleosynthetic ^{20}Ne/^{22}Ne ratios in the He/C zone of supernovae (Rauscher et al. 2002; Chieffi & Limongi 2004) ∼10× more radiogenic Ne, then nucleosynthetic Ne would need to be present in the grain to explain the ratio measured in grain 34-4. Except for the He/C zone, the nucleosynthetic ^{20}Ne/^{22}Ne ratios are well above unity throughout most of the supernova (see, e.g., Figure 4). This makes it difficult to explain low ^{20}Ne/^{22}Ne ratios without having a mixing ratio of radiogenic to nucleosynthetic ^{22}Ne up to several orders of magnitude higher than mentioned above. Considering the overabundance of ^{22}Ne compared with ^{22}Na in a supernova, we would have to invoke a scenario where implanted nucleosynthetic Ne has been partially lost, e.g., by sputtering (see above).

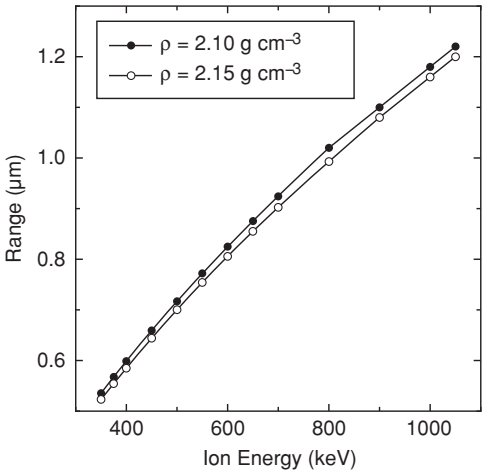

Figure 5. Implantation range vs. ion energy in graphites from the KFB1 density fraction (density $\rho = 2.10$–2.15 g cm^{-3}). The implantation ranges were obtained by SRIM simulation assuming an ion energy range based on high-velocity wind observations in planetary nebulae (see text).

KFB1g 45-1 is the only grain besides 34-4 where ^{20}Ne and ^{22}Ne, but no ^{4}He, has been detected. Its ^{20}Ne/^{22}Ne ratio of 1.7 ± 1.0 is considerably higher than current AGB star He-shell model predictions, but has a large uncertainty. The grain's ^{20}Ne/^{22}Ne ratio is between the predicted ranges for ONe and CO nova neon (Figure 6), but its ^{12}C/^{13}C ratio (15.9 ± 0.1) is higher than predicted and observed in SiC grains with putative nova origins. Also, the inferred ^{26}Al/^{27}Al ratio ($\leqslant 0.6 \times 10^{-3}$) is lower than nova model yields (José & Hernanz 2007) and would require dilution with >90% of contaminating Al (see Section 3.4). This grain also has a negative δ^{25}Mg value (−75 ± 33 ‰), inconsistent with any nova model predictions (δ^{25}Mg range from ∼800‰ to ∼400,000‰; José et al. 2004). The C-isotopic composition, on the other hand, is consistent with an origin from a 15 $M_{\odot}$ supernova if matter from the He/N- and H-zones is mixed in a ratio 2:1 which gives ^{12}C/^{13}C = 16. But the calculated ^{26}Al/^{27}Al ratio of 0.026 is still very high and would require dilution with >75% normal Al and the predicted ^{25}Mg/^{24}Mg ratio of 0.8× solar is lower than observed and would require ∼50% of contaminating Mg. The ^{20}Ne/^{22}Ne ratio of 1.7 ± 1.0 is difficult to explain in the context of a supernova origin; however, its large error does not allow to set strong constraints. A qualitative ad hoc explanation is the implantation of He/N and H zones Ne (^{20}Ne/^{22}Ne ≈ 19; Figure 4) into the grain that already contains Ne-R. This implies this particular grain did not

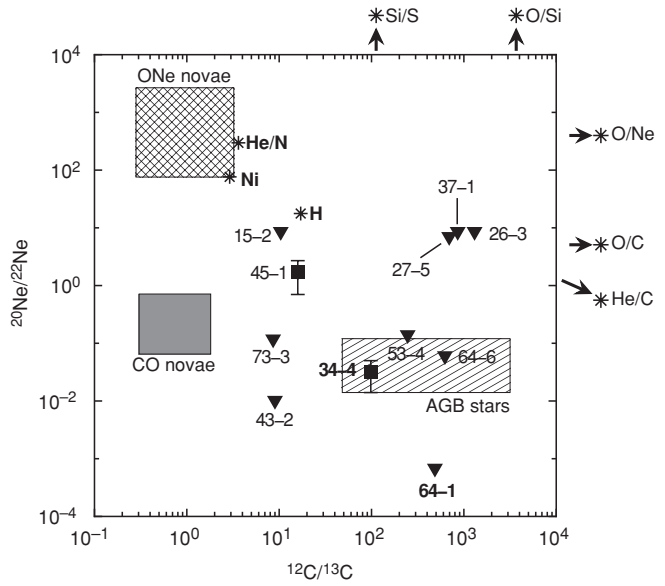

Figure 6. ^{20}Ne/^{22}Ne and ^{12}C/^{13}C ratios of the KFB1 graphite grains studied here. Black squares are shown for the two grains where both ^{20}Ne and ^{22}Ne was detected. All other ^{22}Ne-rich grains are represented as triangles and are upper limits of the ^{20}Ne/^{22}Ne ratio. Model predictions of different stellar sources are shown as shaded areas. Supernova model yields (from Rauscher et al. 2002) are averaged for different supernova zones (see text) and are indicated as asterisks labeled to the right. AGB star predictions are from the latest Torino model (Heck et al. 2007) and nova predictions are from José et al. (2004) in all figures. Errors are 1σ analytical uncertainties based on counting statistics and are shown if larger than symbols in all figures.

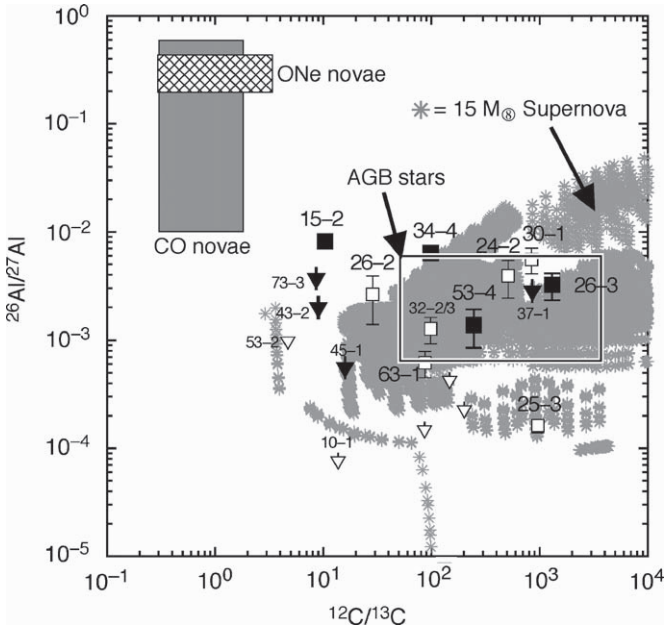

Figure 7. ^{12}C/^{13}C ratios and inferred ^{26}Al/^{27}Al ratios of the subset of grains where ^{26}Al/^{27}Al ratios or upper limits could be determined from the analysis of the melt residue. Black squares designate >2σ evidence for extinct ^{26}Al; upper limits for ^{26}Al/^{27}Al are shown as triangles. Full symbols designate ^{22}Ne-rich grains and open symbols ^{22}Ne-poor grains. Although the predictions for the 15 $M_{\odot}$ supernova model overlap with most of our grain data in this diagram, they do not match in the three-dimensional Ne-C-Al-isotope space.

suffer the same sputtering effect as the other supernova graphite grains.

Grain 26-2 is the only grain in our data set with a considerable enrichment in ^{18}O (^{16}O/^{18}O $\approx$ 302; Table 2). Its ^{18}O-enrichment alone suggests a supernova origin, since the He/C zone of supernovae is strongly enriched in ^{18}O (Rauscher et al. 2002). However, (equilibrium) condensation from the He/C zone would result in a very high (>10^5) ^{12}C/^{13}C ratio in the grain which is not observed (^{12}C/^{13}C = 28.6). A supernova origin can be explained by nonequilibrium condensation and mixing matter from the O/Si, O/Ne, O/C, He/C, He/N, and H zones in a ratio 0.03:0.12:0.04:0.09:0.08:0.65 which gives ^{16}O/^{18}O = 300, ^{12}C/^{13}C = 30, and ^{26}Al/^{27}Al = 0.0038, and is in reasonably good agreement with the grain data. No Ne or He has been detected in this grain.

In summary, the noble gas data, in conjunction with other isotope data, have allowed us to identify one graphite grain with a likely supernova origin (64-1). Data for the other grains discussed above do not place such strong constraints but would allow origins in mixed supernova ejecta.

4.2.2. He-shell Ne and Graphite Grains from AGB Stars

In AGB stars, graphite starts to condense at a temperature of 1600 K under equilibrium and typical atmosphere conditions (C/O = 1.05, $p = 10^{-5}$ bar; Lodders & Fegley 1995). A decrease of ^{22}Ne concentration with increasing grain size was observed and modeled by Verchovsky et al. (2004) in bulk SiC samples measured by Lewis et al. (1994) and in individual presolar SiC grains from AGB stars (Heck et al. 2007). The gas concentration pattern was matched with the SRIM model results, simulating ion implantation into the circumstellar dust grains by a fast, post-AGB star wind. Using this model code, we determined the stopping depths of ^{22}Ne ions in graphite grains (Figure 5). Very fast winds in post-AGB stars have been observed spectroscopically (e.g., up to 2300 km s^{-1}; Sanchez Contreras & Sahai 2001). We assume the same energy range (700 $\pm$ 350 keV for ^{22}Ne) of a fast post-AGB star wind as Verchovsky et al. (2004) and obtain stopping depths of ~0.5–1.2 μm (Figure 5). Within the size range of the analyzed samples (ø 1.7–6.2 μm), these ^{22}Ne ion-stopping depths result in a ^{22}Ne-enrichment near the grain surface as observed for some of the KFB1 graphite grains (Figure 3). Therefore, ion implantation from fast post-AGB star winds is a likely trapping mechanism for Ne in these grains, which formed during the AGB phase. An independent argument for ion implantation in one case is the fact that we have observed both ^{22}Ne and ^{20}Ne, as well as ^{4}He in grain 34-4, the most promising candidate for an AGB star origin. ^{22}Na is not produced in AGB stars and the fact that we observe predominantly ^{22}Ne is due to high mass loss rates during the AGB phase leading to loss of the ^{20}Ne-rich envelope and exposure of the ^{22}Ne-rich He-shell (Gallino et al. 1990; Verchovsky et al. 2004; Heck et al. 2007).

Our most remarkable sample graphite grain KFB1g 34-4 not only contained the highest amount of ^{22}Ne but also allowed us to detect ^{20}Ne and ^{4}He. The Ne, C, and Al isotopic compositions of the grain (^{20}Ne/^{22}Ne = [3.2 $\pm$ 1.8] $\times$ 10^{-2}; ^{12}C/^{13}C = 98.2 $\pm$ 0.8; ^{26}Al/^{27}Al = [6.3 $\pm$ 0.9] $\times$ 10^{-3}) are consistent with predictions for AGB stars with M = 1.5–2 $M_{\odot}$ and 1/2 solar metallicity (Figures 6 and 7; see also Table 4 of Heck et al. 2007; Figure 6 of Zinner et al. 2007). The measured ^{16}O/^{18}O ratio (489 $\pm$ 21) of the grain is normal (as for most other grains) and reflects probably dilution with solar system material (see Section 3.1). The ^{12}C/^{13}C ratio of grain 34-4 excludes a nova origin. The presence of detectable amounts of ^{4}He—despite some He-loss (see Section 4.1)—can also be explained with an AGB star origin involving ion implantation of He-shell material in the post-AGB phase, where the H envelope has been already lost, into circumstellar grains. In this case, the Ne represents

pure Ne-G and no Ne-R is expected to be present. If so, the composition of Ne-G calculates to a $^{20}Ne/^{22}Ne$ ratio of $[3.2 \pm 1.8] \times 10^{-2}$. This is roughly comparable with the $^{20}Ne/^{22}Ne$ ratio of Ne-G ($^{20}Ne/^{22}Ne = 8 \times 10^{-2}$) determined from bulk SiC data (Lewis et al. 1994) and consistent with recent AGB star model predictions (Heck et al. 2007).

4.2.3. Graphite Grains with Low $^{12}C/^{13}C$ Ratios

The C isotopic compositions (Figure 7) of seven grains (10-1, 15-2, 43-2, 53-2, 56-1, 57-3, and 73-3) fall into the range of presolar AB-type SiC grains (Amari et al. 2001b; Zinner et al. 2007). A supernova origin for presolar SiC grains with low $^{12}C/^{13}C$ ratios has been discussed by Nittler & Hoppe (2005) and a nova origin by Amari et al. (2001a). However, most of the SiC grains with low $^{12}C/^{13}C$ ratios are thought to originate from J-type carbon stars (Hoppe et al. 1994, 1996) or born-again AGB stars (Amari et al. 2001b). J-type carbon stars are solar metallicity stars characterized by strong enrichments in ^{13}C leading to low $^{12}C/^{13}C$ ratios (<15) and enrichments in Li. Abundances of *s*-process elements in J-type carbon star photospheres are nearly normal (e.g., Abia & Isern 2000). Since there is no enrichment of *s*-process elements, we speculate that there is also no enrichment in ^{22}Ne, since the latter is also a product of He-shell nucleosynthesis which would be dredged up to the surface. The characteristics of J-type carbon stars cannot be explained by standard AGB star models, and extra mixing processes have to be invoked, depending on stellar mass (Abia & Isern 2000). Extra mixing and processing of envelope material can also occur in AGB stars (cool bottom processing, CBP) and can lead to low $^{12}C/^{13}C$ ratios. However, CBP models of AGB stars do not yield $^{12}C/^{13}C < 12$ and $C/O > 1$ at the same time (Nollet et al. 2003). The nonequilibrium condensation of graphite in AGB stars does not seem to be reasonable because there is no mechanism to dissociate the CO molecule if $C/O < 1$. Hence, we do not consider AGB stars with CBP to be plausible sources of graphites with low $^{12}C/^{13}C$ ratios. Born-again AGB stars occur in a later stage of stellar evolution, during the late post-AGB phase. In this case, the star experiences a very late He-flash whereby the H-envelope is ingested and burned. Dredge up enriches the stellar surface with the burning products, namely, C, N, O, and Ne (in particular ^{22}Ne), and *s*-process elements (e.g., Werner & Herwig 2006). It has been speculated that ^{22}Ne-rich SiC grains of type AB might also be enhanced in *s*-process element abundances and hence might originate from born-again AGB stars (Heck et al. 2007). This could also be the case for gas-rich presolar graphite grain 15-2, which has the highest inferred $^{26}Al/^{27}Al$ ratio $(8.17 \pm 0.86) \times 10^{-3}$, consistent with what is observed for AB type SiC grains (Zinner et al. 2007), and ^{22}Ne-rich grains 43-2 and 73-3. A born-again AGB star origin has also been proposed for four high-density graphite grains from the meteorite Orgueil (Jadhav et al. 2008). In contrast to these three grains, the low-$^{12}C/^{13}C$-grains 10-1, 53-2, 56-1, and 57-3 are ^{22}Ne-poor (i.e., ^{22}Ne is below our detection limit), and, using the same speculation, these grains could then originate from J-type carbon stars. Grain 10-1 has a negative $\delta^{25}Mg$ value ($-98 \pm 29‰$), which would be consistent with an origin in a low-metallicity star (Zinner et al. 2005).

However, very low $^{12}C/^{13}C$ ratios are also characteristic of all nova models (Figures 6 and 7), and also a supernova origin can be invoked for grains with low $^{12}C/^{13}C$ ratios (Nittler & Hoppe 2005). For grains 15-2, 43-2, and 73-3, we have discussed the possibility of a supernova origin. In the following, we will also discuss a nova origin for grains with very low $^{12}C/^{13}C$ ratios. In novae, a low $^{12}C/^{13}C$ ratio (<3) is produced by *p*-capture on ^{12}C to form ^{13}C: $^{12}C(p, \gamma)^{13}N(\beta^+)^{13}C$ (José et al. 2004). It is reasonable to assume that the presolar graphite grains were contaminated with some terrestrial C during the extraction or sample preparation process (Heck et al. 2007), which would increase measured $^{12}C/^{13}C$ ratios. Also, SiC grains with putative nova origins are known to have $^{12}C/^{13}C$ ratios of up to 10 (José & Hernanz 2007). Thus, it is not unrealistic to speculate that the grains with very low $^{12}C/^{13}C$ ratios in particular grains 56-1 ($^{12}C/^{13}C = 4.0$), 53-2 ($^{12}C/^{13}C = 4.7$), and 57-3 ($^{12}C/^{13}C = 5.0$) originated from CO novae (Figures 6 and 7). We note, however, that the upper limit of the $^{26}Al/^{27}Al$ ratio in grain 53-2 ($\leqslant 10^{-3}$) is more than an order of magnitude lower than nova model predictions (José & Hernanz 2007), which would require dilution with >90% of normal Al (see Section 3.4). So far, only two other ^{22}Ne-rich putative nova grains have been reported (José et al. 2004; Heck et al. 2007). The upper limit of the $^{20}Ne/^{22}Ne$ ratios of grain 43-2 (1×10^{-2}) is very low for a nova origin. Predictions for CO novae yield $^{20}Ne/^{22}Ne$ ratios 0.1–0.7, whereas ONe novae have $^{20}Ne/^{22}Ne$ ratios ranging from 90 to 2900; these predicted ratios include nucleosynthetic Ne and radiogenic ^{22}Ne (José & Hernanz 2007). For grain 73-3 the upper limit on $^{20}Ne/^{22}Ne$ (1×10^{-1}) is compatible with an origin from a CO nova. In the context of a nova origin, the inferred $^{26}Al/^{27}Al$ ratio of grain 73-3 also favors a CO nova rather than an ONe nova (Figure 7).

4.2.4. Other Grains

The isotope data of ^{22}Ne-rich grains 26-3, 27-5, 37-1, 53-4, and 64-6 do not allow us to distinguish between a supernova or an AGB star origin. All of them have upper limits of $^{20}Ne/^{22}Ne$ ratios too high (8.6, 7.0, 8.6, 0.1, and 0.06, respectively) to exclude Ne-G and their ^{22}Ne-concentration/diameter ratios are consistent with the He-shell ^{22}Ne-implantation scenario outlined above (Figure 3). However, it would also be possible that we observe Ne-R. Also, the $^{12}C/^{13}C$ and inferred $^{26}Al/^{27}Al$ ratios are consistent with both AGB star and supernova origins. Either an AGB star or supernova origin is also likely for 35 other grains (Table 2). Ne-rich grain 27-5 has a negative $\delta^{25}Mg$ value and has a $^{12}C/^{13}C$ ratio (693), which falls into the range of group-4 grains (Hoppe et al. 1995). The $^{12}C/^{13}C$ ratio is consistent with what is observed for SiC X and Y grains. The SiC Y grains are thought to originate from low-mass AGB stars which experienced strong He shell dredge up (Hoppe et al. 1994). The presence of ^{22}Ne would be consistent with enhanced dredge up. The negative $\delta^{25}Mg$ would be consistent with predictions of C-rich envelopes of low-metallicity, low-mass AGB stars (Zinner et al. 2005). Both the high $^{12}C/^{13}C$ ratio and the low $\delta^{25}Mg$ value could also be explained by mixing of supernova ejecta. In that case, the measured Ne would be radiogenic.

5. CONCLUSIONS

1 We detected excess ^{22}Ne in 11 out of 51 presolar graphite grains (i.e., in 22%) from the KFB1 fraction from the carbonaceous chondrite Murchison. The current fraction, while smaller, is statistically indistinguishable from Nichols et al.'s (1992) fraction of ^{22}Ne-rich KFB1 grains (~30%).

2 Apart from ^{22}Ne, in one 2-micron-sized graphite grain (KFB1g 34-4) ^{20}Ne was above detection limit. The isotope ratios of $^{20}Ne/^{22}Ne$, $^{12}C/^{13}C$, and inferred $^{26}Al/^{27}Al$ imply that KFB1g 34-4 most likely formed in the wind of an AGB

star and trapped He-shell Ne by implantation in the very high speed post-AGB star wind. The $^{20}Ne/^{22}Ne$ ratio of $[3 \pm 2] \times 10^{-2}$ is consistent with predictions for He-shells of AGB stars with 1.5–2 $M_{\odot}$ and 1/2 solar metallicity.

3 We report unequivocal evidence that one presolar graphite grain (KFB1g 64-1) contains radiogenic ^{22}Ne (Ne-R), and condensed in a supernova where it incorporated live ^{22}Na and inherited the C isotopic composition of a mixture of different supernova zones. The upper limit of its $^{20}Ne/^{22}Ne$ ratio is 7×10^{-4}. We conclude that nonradiogenic Ne in supernova grains is very rare because either it was not implanted at all or has been lost presumably by sputtering of the grain surface in the supernova ejecta.

4 Presolar KFB1 graphite grains lost considerably more of their ^{4}He than presolar SiC grains. ^{4}He was detected only in 1 out of 51 graphite grains and the He/Ne ratio is too low to be considered as unfractionated. The weak retentivity of graphite grains for He explains the nondetection of He in most graphite grains.

5 Born-again AGB stars (^{22}Ne-rich grains), J-type carbon stars (^{22}Ne below detection limit), CO novae, and supernovae are potential stellar sources for the six grains with $^{12}C/^{13}C$ ratios $<\sim 10$.

6 Isotopic data of the remaining 40 grains, three of them are ^{22}Ne-rich, exclude low $^{12}C/^{13}C$ sources (i.e., born-again AGB stars, J-type C-stars and novae). Thus, they originate either from AGB stars or from supernovae.

Future single grain noble gas studies of presolar graphite grains will enlarge the database and sharpen our understanding of these fascinating stellar samples and might be performed in conjunction with SIMS analyses of Si-isotopes to set tighter constraints on the grains' stellar sources.

We thank E. Gröner for technical assistance with the NanoSIMS in Mainz, J. Huth for his support with SEM, and M. Meier for his assistance with noble gas measurements. We thank A. Heger for his permission to use supernova yield predictions from nucleosynthesis.org. We also thank an anonymous referee for critical, constructive comments that greatly helped to improve the manuscript. This project has been supported by NASA grants NNX09AG39G (P.R.H.; P. I.: A. M. Davis) and NNX08AG56G (S.A.), and was partially funded by ETH Zurich and the Swiss National Science Foundation (R.W.).

REFERENCES

Abia, C., & Isern, J. 2000, ApJ, 536, 438
Amari, S. 2006, New Astron. Rev., 50, 578
Amari, S. 2009, ApJ, 690, 1424
Amari, S., Anders, E., Virag, A., & Zinner, E. 1990, Nature, 345, 238
Amari, S., Gao, X., Nittler, L. R., Yinner, E., José, J., Hernanz, M., & Lewis, R. S. 2001a, ApJ, 551, 1065
Amari, S., Hoppe, P., Zinner, E., & Lewis, R. S. 1992, ApJ, 394, L43
Amari, S., Lewis, R., & Anders, E. 1994, Geochim. Cosmochim. Acta, 58, 489
Amari, S., Lewis, R., & Anders, E. 1995, Geochim. Cosmochim. Acta, 59, 1411
Amari, S., Nittler, L. R., Zinner, E., Lodders, K., & Lewis, R. S. 2001b, ApJ, 559, 463
Amari, S., Zinner, E., & Lewis, R. S. 1996, ApJ, 470, L101
Asher, R. C., & Wilson, S. A. 1958, Nature, 181, 409
Baur, H. 1999, EOS Trans., 46, F1118
Besmehn, A., & Hoppe, P. 2003, Geochim. Cosmochim. Acta, 67, 4693
Black, D. C., & Pepin, R. O. 1969, EPSL, 6, 395
Chieffi, A., & Limongi, M. 2004, ApJ, 608, 405
Clayton, D. D., & Hoyle, F. 1974, ApJ, 187, L101
Clayton, D. D. 1975, Nature, 257, 36
Clayton, D. D., Liu, W., & Dalgaro, A. 1999, Science, 283, 1290
Croat, T. K., Stadermann, F. J., & Bernatowicz, T. J. 2005, ApJ, 631, 976
Croat, T. K., Stadermann, F. J., & Bernatowicz, T. J. 2008, Meteoritics Planet. Sci., 43, 1497
Deneault, E. A.-N., Clayton, D. D., & Heger, A. 2003, ApJ, 594, 312
Deneault, E. A.-N., Clayton, D. D., & Meyer, B. S. 2006, ApJ, 638, 234
Ebel, D. S., & Grossman, L. 2001, Geochim. Cosmochim. Acta, 65, 469
Eberhardt, P., Eugster, O., & Marti, K. 1965, Z Naturforsch, 20, 623
Eberhardt, P., Jungck, M. H. A., Meier, F. O., & Niederer, F. R. 1981, Geochim. Cosmochim. Acta, 45, 1515
Gallino, R., Busso, M., Picchio, G., & Raiteri, C. M. 1990, Nature, 348, 298
Gehrz, R. D., Truran, J. W., Williams, R. E., & Starrfield, S. 1998, PASP, 110, 3
Heck, P. R., Marhas, K. K., Hoppe, P., Gallino, R., Baur, H., & Wieler, R. 2007, ApJ, 656, 1208
Hoppe, P., Amari, S., Zinner, E., Ireland, T., & Lewis, R. S. 1994, ApJ, 430, 870
Hoppe, P., Amari, S., Zinner, E., & Lewis, R. S. 1995, Geochim. Cosmochim. Acta, 59, 4029
Hoppe, P., Strebel, R., Eberhardt, P., Amari, S., & Lewis, R. S. 1996, Geochim. Cosmochim. Acta, 60, 883
Hoppe, P., Strebel, R., Eberhardt, P., Amari, S., & Lewis, R. S. 2000, Meteoritics Planet. Sci., 35, 1157
Jadhav, M., Amari, S., Marhas, K. K., Zinner, E., Maruoka, T., & Gallino, R. 2008, ApJ, 682, 1479
José, J., & Hernanz, M. 2007, Meteoritics Planet. Sci., 42, 1135
José, J., Hernanz, M., Amari, S., Lodders, K., & Zinner, E. 2004, ApJ, 612, 414
Kehm, K., Amari, S., Hohenberg, C. M., & Lewis, R. S. 1996, Lunar Planet. Sci. Conf., 27, 657
Lewis, R., Amari, S., & Anders, E. 1994, Geochim. Cosmochim. Acta, 58, 471
Lodders, K., & Fegley, B. 1995, Meteoritics, 30, 661
Limongi, M., & Chieffi, A. 2003, ApJ, 592, 404
Mamyrin, B. A., Anufriev, G. S., Kamenskii, I. L., & Tolstikhin, I. N. 1970, Geochem. Int., 7, 498
Meyer, B. S., Weaver, T. A., & Woosley, S. E. 1995, Meteoritics Planet. Sci., 30, 325
Nath, B., Laskar, T., & Shull, M. 2008, ApJ, 682, 1055
Nichols, R. H., Jr., Hohenberg, C. M., Hoppe, P., Amari, S., & Lewis, R. S. 1992, Lunar Planet. Sci. Conf., 23, 989
Nichols, R. H., Jr., Kehm, K., Brazzle, R., Amari, S., Hohenberg, C. M., & Lewis, R. S. 1994, Meteoritics, 29, 510
Nittler, L. R., Amari, S., Zinner, E., Woosley, S. E., & Lewis, R. S. 1996, ApJ, 462, L31
Nittler, L. R., & Hoppe, P. 2005, ApJ, 631, L89
Nollet, K. M., Busso, M., & Wasserburg, G. J. 2003, ApJ, 582, 1036
Nozawa, T., Kozasa, T., Habe, A., Dwek, E., Umeda, H., Tominaga, N., Maeda, K., & Nomoto, K. 2007, ApJ, 666, 955
Nozawa, T., Kozasa, T., Umeda, H., Maeda, K., & Nomoto, K. 2003, ApJ, 598, 785
Rauscher, T., Heger, A., Hoffman, R. D., & Woosley, S. E. 2002, ApJ, 576, 323
Rho, J., Kozasa, T., Reach, W. T., Smith, J. D., Rudnick, L., DeLaney, T., Ennis, J. A., Gomez, H., & Tappe, A. 2008, ApJ, 673, 271
Sanchez Contreras, C., & Sahai, R. 2001, ApJ, 552, L173
Travaglio, C., Gallino, R., Amari, S., Zinner, E., Woosley, S., & Lewis, R. S. 1999, ApJ, 510, 325
Verchovsky, A. B., Wright, I. P., & Pillinger, C. T. 2004, ApJ, 607, 611
Werner, K., & Herwig, F. 2006, PASP, 118, 183
Yoshida, T. 2007, ApJ, 666, 1048
Ziegler, J. F. 2004, Nucl. Instr. Meth. Phys. Res. B, 219–220, 1027
Zinner, E. K. 2004, in Meteorites, Comets, and Planets, Vol. 1, Treatise in Geochemistry, ed. A. M. Davis, H. D. Holland, & K. K. Turekian , (1st ed.; Oxford: Elsevier), 17
Zinner, E., et al. 2007, Geochim. Cosmochim. Acta, 71, 4786
Zinner, E., Nittler, L. R., Hoppe, P., Gallino, R., Straniero, O., & Alexander, C. M. O'D. 2005, Geochim. Cosmochim. Acta, 60, 4149